Bioconjugate Chemistry

Article

pubs.acs.org/bc

PEG-Farnesylthiosalicylate Conjugate as a Nanomicellar Carrier for Delivery of Paclitaxel

Xiaolan Zhang,[†,‡,§] Jianqin Lu,[†,‡,§] Yixian Huang,[†,‡,§] Wenchen Zhao,[‡] Yichao Chen,[†,‡,§] Jiang Li,[†,‡,§] Xiang Gao,[†,‡,§] Raman Venkataramanan,[‡] Ming Sun,[∥] Donna Beer Stolz,[∥] Lin Zhang,[§,⊥] and Song Li*[,†,‡,§]

[†]Center for Pharmacogenetics, [‡]Department of Pharmaceutical Sciences, School of Pharmacy, and [§]University of Pittsburgh Cancer Institute, University of Pittsburgh, Pittsburgh, Pennsylvania 15261, United States

[∥]Department of Cell Biology and Physiology, [⊥]Department of Pharmacology and Chemical Biology, University of Pittsburgh School of Medicine, Pittsburgh, Pennsylvania 15261, United States

Supporting Information

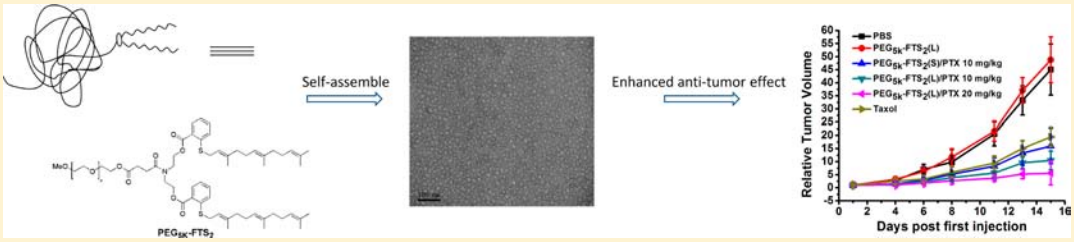

ABSTRACT: S-trans, trans-farnesylthiosalicylic acid (FTS) is a synthetic small molecule that acts as a potent and especially nontoxic Ras antagonist. It inhibits both oncogenically activated Ras and growth factor receptor-mediated Ras activation, resulting in the inhibition of Ras-dependent tumor growth. In this work, an FTS conjugate with poly(ethylene glycol) (PEG) through a labile ester linkage, PEG_{5K}-FTS_2(L), was developed. PEG_{5K}-FTS_2 conjugate readily forms micelles in aqueous solutions with a critical micelle concentration of 0.68 μM, and hydrophobic drugs such as paclitaxel (PTX) could be effectively loaded into these particles. Both drug-free and PTX-loaded micelles were spherical in shape with a uniform size of 20−30 nm. The release of PTX from PTX-loaded PEG_{5K}-FTS_2 micelles was significantly slower than that from Taxol formulation. *In vitro* cytotoxicity studies with several tumor cell lines showed that PEG_{5K}-FTS_2(L) was comparable to FTS in antitumor activity. Western immunoblotting showed that total Ras levels were downregulated in several cancer cell lines treated with FTS or PEG_{5K}-FTS_2(L). The micellar formulation of PTX exhibited more *in vitro* cytotoxic activity against several tumor cell lines compared with free PTX, suggesting a possible synergistic effect between the carrier and the codelivered drug. The antitumor activity of the PTX loaded PEG_{5K}-FTS_2(L) micelles in a syngeneic murine breast cancer model was found to be significantly higher than that of Taxol, which may be attributed to their preferential tumor accumulation and a possible synergistic effect between PEG_{5K}-FTS_2 carrier and loaded PTX.

INTRODUCTION

Clinical application of PTX in cancer therapy is limited by problems such as low water solubility, lack of tissue-specificity, and high toxicity.[1,2] A number of macromolecular delivery systems are under investigation to circumvent these limitations and improve the potential of the anticancer drug.[3,4] However, it remains a challenge to design a vehicle that can carry sufficient amounts of drugs and efficiently overcome various physiological barriers to reach the tumor tissues.[5] Micelles with a nanoscopic supramolecular core−shell structure are one such carrier of choice. It has been established that a nanocarrier with the size of 20−100 nm preferentially extravasates into solid tumor tissues owing to the leaky tumor vasculature.[6−8] Additionally, a hydrophilic polymer (PEG) grafted onto the surface prolongs blood circulation times of the micelles due to the inhibition of nonspecific uptake by reticuloendothelial system (RES).[9,10] However, for most delivery systems, vehicles themselves rarely possess pharmacological activity. The use of "inert" excipients that lack therapeutic activity not only adds to the cost, but also potentially imposes safety issues.[11]

An interesting strategy in the design of multifunctional nanocarriers is the use of a highly water-insoluble drug itself as the hydrophobic region of polymeric micelles. One example is pegylated vitamin E, D-α-tocopheryl poly(ethylene glycol) succinate (Vitamin E TPGS or TPGS).[12−14] Vitamin E itself shows antitumor effect against different types of cancers, and vitamin E TPGS is effective in solubilizing various hydrophobic drugs. Synergistic effects between the TPGS-based carriers and delivered anticancer drugs have been demonstrated.[15]

Recently, our group reported another dual-functional carrier that is based on PEG-derivatized embelin.[16,17] Embelin shows antitumor activity in various types of cancers through various

Received: November 14, 2012
Revised: January 28, 2013
Published: February 20, 2013

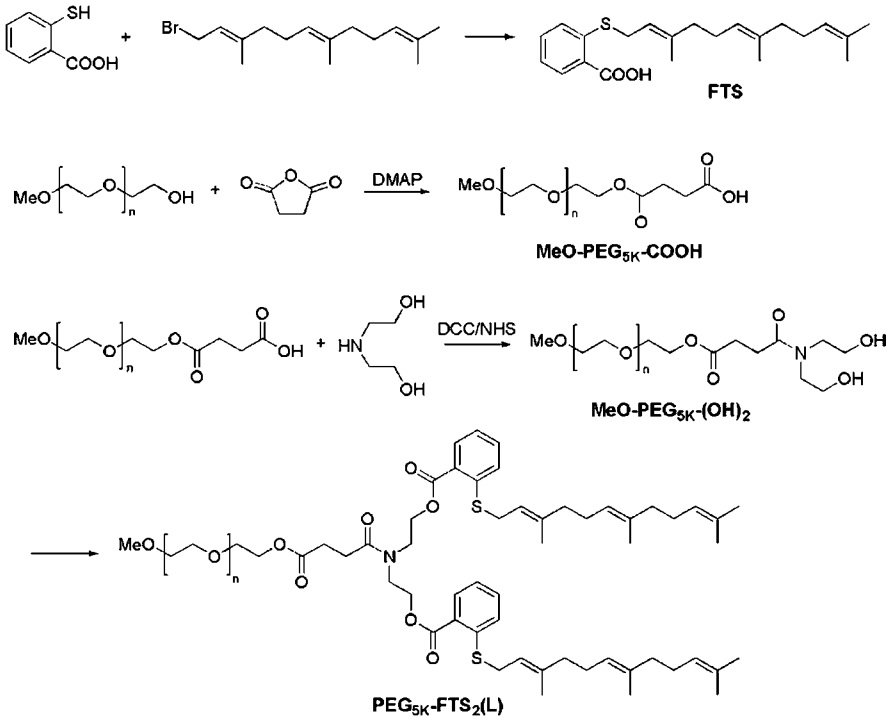

Figure 1. Synthesis scheme of PEG_{5K}-FTS_2(L) conjugate.

mechanisms such as the inhibition of the activity of X-linked inhibitor of apoptosis protein (XIAP).[18] PEG-modified embelin shows significantly increased solubility (>200 mg/mL) in aqueous solution. More importantly, PEG-embelin forms micelles that effectively solubilize various types of hydrophobic drugs such as PTX. Significantly improved antitumor efficacy was demonstrated for PTX formulated in PEG-embelin micelles both *in vitro* and *in vivo*.[16,17]

In this study, we design a self-assembling nanomicellar system that is based on PEG-derivatized farnesylthiosalicylic acid (FTS) for targeted delivery of PTX. FTS is a first-in-class direct Ras antagonist designed to inhibit overactive cell growth in cancers caused by various Ras proteins.[19,20] Permanently active Ras caused by mutation in the Ras family of proto-oncogenes is present in one-third of human cancers, with the highest incidence of mutational activation of Ras being detected in pancreatic (90%) and colon (50%) cancers.[21,22] FTS has demonstrated significant reduction of Ras levels in a wide array of established cancer models without observable side effects.[23] One major mechanism involves affecting membrane interaction by inducing dislodgement of ras protein from its anchorage domains, facilitating its degradation, and thus disrupting ras protein to signal in the plasma membrane.[24,25] FTS is poorly water-soluble[26] and PEGylation is designed to improve its solubility. At the same time, PEG-FTS conjugate forms micelles, which could be applied as an ideal carrier for hydrophobic drugs to improve the efficiency and safety profile. Additionally, the carrier materials can potentially promote synergistic effects with the codelivered anticancer drug. The PEG_{5K}-FTS_2 conjugate was synthesized and characterized for its structure and molecular weight. We further characterized the biophysical properties of drug-loaded micelles including particle size, loading capacity, and *in vitro* drug release kinetics. Finally, the *in vitro* and *in vivo* antitumor activity of PTX/PEG-FTS was investigated.

EXPERIMENTAL PROCEDURES

Materials. Paclitaxel (98%) was purchased from AK Scientific Inc. (CA, USA). FTS was synthesized and purified following the published literature.[20] Pan-Ras Ab (Ab-3) was purchased from Calbiochem (La Jolla, CA). HRP-labeled goat antimouse IgG and the ECL chemiluminescence kit were purchased from Amersham Biosciences (Piscataway, NJ, USA). Dulbecco's phosphate buffered saline (DPBS) was purchased from Lonza (MD, USA). Poly(ethylene glycol) methyl ether (MeO-PEG-OH, M_w = 5000 kDa), dimethyl sulfoxide (DMSO), 3-(4,5-dimethylthiazol-2-yl)-2,5-diphenyl tetrazolium bromide (MTT), trypsin-EDTA solution, Triton X-100, and Dulbecco's Modified Eagle's Medium (DMEM) were all purchased from Sigma-Aldrich (MO, USA). Fetal bovine serum (FBS) and penicillin–streptomycin solution were from Invitrogen (NY, USA).

Synthesis of PEG_{5K}-FTS_2(L) and PEG_{5K}-FTS_2(S) Conjugate. PEG_{5K}-FTS_2(L) conjugate with a labile linkage was prepared via solution-phase condensation reactions from MeO-PEG-OH with a molecular weight of 5000 (Figure 1). We started by synthesizing carboxyl terminated PEG monomethyl ether (MeO-PEG_{5k}-COOH) from MeO-PEG_{5k}-OH (1 equiv) by a facile chemical reaction with succinic anhydride (5 equiv) and 4-(dimethylamino) pyridine (DMAP 5 equiv) in pyridine according to a reported method.[27] To obtain two hydroxyl group terminated PEG monomethyl ether (MeO-PEG_{5k}-$(OH)_2$), diethanolamine (3 equiv) was coupled onto the carboxylic group of MeO-PEG_{5k}-COOH (1 equiv) using *N*-hydroxysuccinimide (NHS 3.6 equiv)/dicyclohexylcarbodiimide (DCC 3.6 equiv) as coupling agent in chloroform overnight. The polymer was precipitated and washed by ice-cold ether three times, and concentrated under vacuum. MeO-PEG_{5k}-$(OH)_2$, FTS, DCC, and DMAP were then dissolved in chloroform with a molar ratio of 1:6:3:0.3 and allowed to react overnight at room temperature. The solution was filtered and

dx.doi.org/10.1021/bc300608h | *Bioconjugate Chem.* 2013, 24, 464–472

precipitated in ice-cold diethyl ether and ethanol twice respectively, and concentrated under vacuum. The powder was then dissolved in water and filtered through a filter with a pore size of 0.2 μm. The final product was obtained by lyophilizing the filtrate. At the same time, we also prepared a PEG_{5K}-FTS_2(S) conjugate (Figure S1) with a stable amide linkage. MeO-PEG_{5k}-OH and (*S*)-2,6-Bis-*tert*-butoxycarbonylaminohexanoic acid (Boc-Lys(Boc)-OH) were dissolved in chloroform together with DCC and DMAP with a molar ratio of 1:3:1.5:0.3 and the mixture was left to react overnight at room temperature. PEGylated molecules were recovered from the mixture through three cycles of dissolution/reprecipitation with chloroform and ether, respectively. Boc groups were removed via the treatment with 50% (v/v) trifluoroacetic acid (TFA) in chloroform, and PEGylated molecules were precipitated and washed with ice-cold ether. Finally, FTS was coupled onto the N terminal group of MeO-PEG_{5k}-Lys-$(NH_2)_2$ (1 equiv) via NHS (3.6 equiv)/DCC (3.6 equiv) as described above. After the reaction was completed, the solution was precipitated in cold ether. PEG_{5K}-FTS_2(S) was similarly purified as that for PEG_{5K}-FTS_2(L).

Preparation of PTX-Loaded and Drug-Free Micelles. PTX (10 mM in chloroform) and PEG_{5K}-FTS_2 (10 mM in chloroform) were mixed with various carrier/drug ratios. The organic solvent was removed by nitrogen flow to form a thin film of drug/carrier mixture. The film was dried under vacuum for 1 h to remove the remaining solvent. DPBS was added to hydrate the thin film and the drug-loaded micelles were formed. Unincorporated PTX (precipitate) was removed by filtering with a syringe filter (pore size: 0.22 μm). The drug-free micelles were similarly prepared as described above.

Characterizations of PTX-Loaded and Drug-Free Micelles. The particle size and zeta potential of micelles were measured by a Zetasizer (DLS) (Zetasizer Nano ZS instrument, Malvern, Worcestershire, UK). The micelle concentrations were kept at 1 mg/mL. The morphology and size distribution of drug-free or PTX-loaded PEG_{5K}-FTS_2 micelles were observed using transmission electron microscopy (TEM). A copper grid with Formvar was used. The copper grid was immersed in a drop of sample solution and stained with 1% uranyl acetate. Imaging was performed at room temperature on JEOL JEM-1011.

The critical micelle concentration (CMC) of PEG_{5K}-FTS_2 was determined using pyrene as a fluorescence probe.[28] PEG_{5K}-FTS_2 was prepared in chloroform at 1.2 mg/mL and various amounts were added to 9 separate vials, respectively. Then, 10 μL of 1.8×10^{-4} M of pyrene in chloroform was added to each vial and the solution was mixed well. The organic solvent was removed by nitrogen flow to form a thin film. Finally, 3 mL Milli-Q water was added to each vial and the final pyrene concentration was 6×10^{-7} M with PEG_{5K}-FTS_2 concentrations ranging from 0.0001 to 0.5 mg/mL. The vials were kept on a shaker at 37 °C for 24 h to reach equilibrium prior to fluorescence measurement. The excitation spectra were scanned from 310 to 350 nm at a fixed emission wavelength of 390 nm by Synergy H1 Hybrid Multi-Mode Microplate Reader (Winooski, VT). The pyrene fluorescence intensity ratio I_{338}/I_{334} in the excitation spectra was analyzed for calculation of CMC.

The drug loading efficiency was quantified by high-performance liquid chromatography (HPLC) (Alliance 2695−2998 system). The reverse-phase Lichrospher 100 RP-18 (5 μm) column was used and the mobile phase consisted of methanol/water (80:20 v/v). The flow rate was set at 0.8 mL/min and the column effluent was detected at 227 nm with a UV/vis detector. Drug loading capacity (DLC) and drug loading efficiency (DLE) were calculated according to the following equation:

$$\text{DLC}(\%) = [\text{weight of drug used}/(\text{weight of polymer} + \text{drug used})] \times 100\%$$

$$\text{DLE}(\%) = (\text{weight of loaded drug}/\text{weight of input drug}) \times 100\%$$

***In Vitro* Drug Release Study.** Release of PTX from PTX-loaded PEG_{5K}-FTS_2 micelles was performed following a method described previously.[16] Briefly, 3 mL of PTX-loaded PEG_{5K}-FTS_2 micelles or Taxol (1 mg PTX/mL) solution was placed in a dialysis bag (MWCO = 12 kDa, Spectrum Laboratories) that was incubated in 200 mL DPBS (PH = 7.4) containing 0.5% (w/v) Tween 80 at 37 °C with gentle shaking. The concentration of PTX remaining in the dialysis tubes at designated time points was measured by HPLC with the detection wavelength at 227 nm. Values were reported as the means from triplicate samples.

Hemolytic Effect of PEG_{5K}-FTS_2 Micelles. Hemolysis assay was performed using fresh blood collected through cardiac puncture from rats. The red blood cells (RBCs) were collected by centrifugation at 1500 rpm for 10 min at 4 °C. After washing three times with PBS, RBCs were diluted at a final concentration of 2% w/v in PBS. One milliliter of diluted RBC suspension was mixed with various concentrations (0.2 and 1.0 mg/mL) of PEG_{5k}-FTS_2 and PEI, respectively, and then incubated at 37 °C in an incubator shaker for 4 h. The mixtures were centrifuged at 1500 rpm for 10 min at 4 °C, and 100 μL of supernatant from each sample was transferred into a 96-well plate. The release of hemoglobin was determined at 540 nm absorbance using a microplate reader. RBCs incubated with Triton X-100 (2%) and PBS were used as the positive and negative controls, respectively. The percentage of hemolysis of RBCs was calculated as $(OD_{sample} - OD_{negative\ control})/(OD_{positive\ control} - OD_{negative\ control}) \times 100\%$.

Cell Culture. DU145 and PC-3 are two androgen-independent human prostate cancer cell lines. 4T1.2 is a mouse metastatic breast cancer cell line. HCT-116 is a human colon carcinoma cell line. All cell lines were cultured in DMEM containing 5% FBS and 1% penicillin−streptomycin at 37 °C in a humidified 5% CO_2 atmosphere.

***In Vitro* Cell Cytotoxicity.** For cytotoxicity measurement, DU145 (2000 cells/well), PC-3 (2000 cells/well), 4T1.2 (1000 cells/well), or HCT-116 (1000 cells/well) were seeded in 96-well plates. After 24 h of incubation in DMEM with 5% FBS and 1% streptomycin−penicillin, the old medium was removed and the cells were incubated for 72 h in the presence of indicated concentrations of PTX (free or formulated in PEG_{5K}-FTS_2 micelles). Twenty microliters of 3-(4,5-dimethylthiazol-2-yl)-2,5-diphenyltetrazoliumbromide (MTT) in DPBS (5 mg/mL) was added to each well and cells were further incubated for 4 h. MTT formazan was solubilized by DMSO. The absorbance in each well was measured by a microplate reader with wavelength at 550 nm and reference wavelength at 630 nm. Untreated groups were used as controls. Cell viability was calculated as $[(OD_{treat} - OD_{blank})/(OD_{control} - OD_{blank}) \times$

dx.doi.org/10.1021/bc300608h | *Bioconjugate Chem.* 2013, 24, 464−472

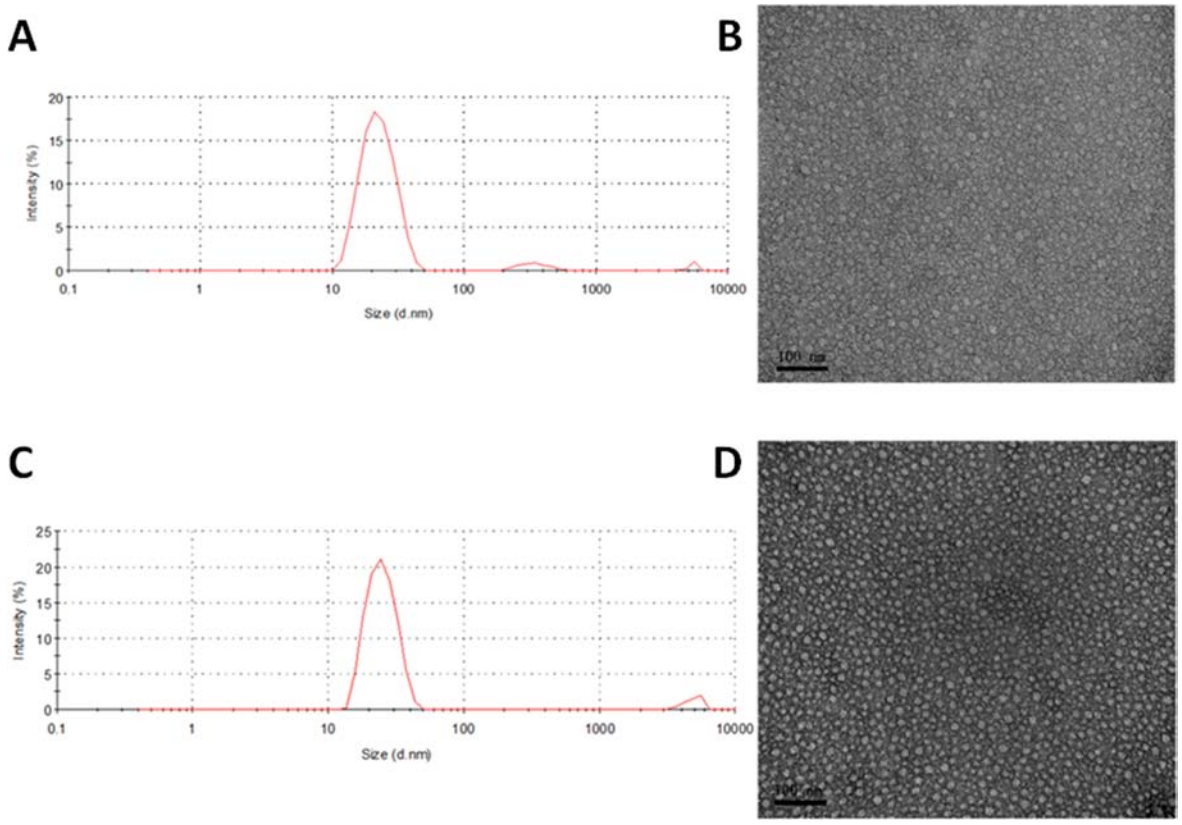

Figure 2. Particle size distribution of drug-free PEG_{5K}-FTS_2 (A) and PTX-loaded PEG_{5K}-FTS_2 micelles (C). TEM images of drug-free PEG_{5K}-FTS_2 (B) and PTX-loaded PEG_{5K}-FTS_2 micelles (D).

100%]. The cytotoxicity of PEG_{5K}-FTS_2(L) or PEG_{5K}-FTS_2(S) alone was similarly examined.

Western Immunoblotting. Cells were grown in dishes in medium containing 5% FBS, in the presence of 0.1% DMSO (control) or indicated concentrations of FTS, PEG_{5K}-FTS_2(L), and PEG_{5K}-FTS_2(S), respectively. Following treatment for 48 h, cells were washed with ice-cold PBS twice and solubilized in lysis buffer. The lysates were centrifuged at 14 000 for 10 min after a 10 min incubation on ice. Samples with equal amounts of total cellular proteins were subjected to 15% sodium dodecylsulfate polyacryl amide gel electrophoresis (SDS-PAGE) before proteins were transferred to nitrocellulose membranes. The membranes were incubated with primary antibody in 5% nonfat dry milk dissolved in DPBS with 0.1% Tween 20 (PBST) overnight at 4 °C. After washing three times with PBST, the membranes were incubated with secondary antibody at a final dilution of 1:10 000 in PBST for 1 h at room temperature. After washing three times with PBST, bound antibodies were detected by chemiluminescence. β-actin was used as a loading control.

Animals. Female BALB/c mice, 10−12 weeks in age, were purchased from Charles River (Davis, CA). All animals were housed under pathogen-free conditions according to AAALAC guidelines. All animal-related experiments were performed in full compliance with institutional guidelines and approved by the Animal Use and Care Administrative Advisory Committee at the University of Pittsburgh.

***In Vivo* Therapeutic Study.**[29,30] A syngeneic murine breast cancer model (4T1.2) was used to examine the therapeutic effect of different formulations of PTX. 1×10^5 4T1.2 cells in 200 μL PBS were inoculated s.c. at the right flank of female BALB/c mice. Treatments were started when tumors in the mice reached a tumor volume of ~50 mm^3, and this day was designated as day 1. On day 1, these mice were randomly divided into six groups (n = 5) and administered i.v. with PBS (control), free PEG_{5K}-FTS_2(S) micelles, Taxol (10 mg PTX/kg), PTX-loaded PEG_{5K}-FTS_2(L) (10 and 20 mg PTX/kg), and PTX-loaded PEG_{5K}-FTS_2(S) (10 mg PTX/kg), respectively, on days 1, 4, 6, 8, 11, and 13. Free PEG_{5K}-FTS_2(L) micelles were given at the equivalent dosage of the carrier in the group of PTX-loaded PEG_{5K}-FTS_2(L) micelles (10 mg PTX/kg). Tumor sizes were measured with digital caliper three times a week and calculated by the formula: $(L \times W^2)/2$, where L is the longest and W is the shortest in tumor diameters (mm). To compare between groups, relative tumor volume (RTV) was calculated at each measurement time point (where RTV equals to the tumor volume at a given time point divided by the tumor volume prior to first treatment). Mice were sacrificed when tumor reached 2000 mm^3.

Statistical Analysis. In all statistical analysis, the significance level was set at a probability of $P < 0.05$. All results were reported as the mean ± standard error (SEM) unless otherwise indicated. Statistical analysis was performed by Student's t test for two groups, and one-way ANOVA for multiple groups, followed by Newman-Keuls test if $P < 0.05$.

RESULTS

Synthesis of PEG_{5K}-FTS_2(L) and PEG5K-FTS2(S) Conjugates. PEG_{5K}-FTS_2(L) conjugate, containing two molecules of FTS coupled to one molecule of PEG via a labile ester linkage, was developed by solution-phase condensation reactions. ^{1}H NMR spectra of PEG_{5K}-FTS_2(L) conjugate are

dx.doi.org/10.1021/bc300608h | *Bioconjugate Chem.* 2013, 24, 464−472

shown in Figure S2A, with signals at 3.63 ppm attributable to the methylene protons of PEG. Carbon chain signals and benzene ring signals of FTS were located at 1.5−2.2 ppm and 7−8 ppm, respectively. A peak appeared at δ 4.5 from $-CH_2CH_2N$ group confirmed the conjugation of FTS with PEG. The signal ratio of the protons on PEG chain to the protons on $-C{=}C(CH_3)_2$ group of FTS is around 1:8 (Figure S2A), which suggested that two FTS molecules were attached onto the PEG chain. The molecular weight of the PEG_{5K}-FTS_2(L) conjugate measured by MALDI-TOF mass spectra is close to the theoretical value (5867) (Figure S3A), further confirming that two FTS molecules were conjugated to one molecule of PEG. HPLC shows that the purity of the final product [PEG_{5K}-FTS_2(L)] is 94.52% (Figure S4A). We also synthesized PEG_{5K}-FTS_2(S) conjugate in which FTS was coupled onto PEG chain via a stable amide linkage. ^{1}H NMR spectra, MALDI-TOF mass spectra, and HPLC (Figures S2B, S3B, and S4B) confirmed the successful synthesis of PEG_{5K}-FTS_2(S) conjugate.

Characterizations of Micelles. The PEG_{5K}-FTS_2 conjugate readily formed micelles in aqueous solution. Dynamic light scattering (DLS) measurements showed that these micelles had hydrodynamic sizes around 22 nm at the concentration of 20 mg/mL (Figure 2A). TEM revealed spherical particles with uniform size distribution (Figure 2B). The size observed by TEM shows good agreement with that determined by DLS. PTX could be effectively loaded into PEG_{5K}-FTS_2 micelles. The size and size distribution were not significantly affected when PTX was loaded into micelles at a drug concentration of 1 mg/mL and a carrier/drug ratio of 5/1 (m/m) (Figure 2C,D).

The CMC of PEG_{5K}-FTS_2 micelles was measured using pyrene as a fluorescence probe. When the concentration of the PEG_{5K}-FTS_2 reached the CMC, there is a major change for the I_{338}/I_{334} value due to the transfer of pyrene from polar microenvironment to nonpolar microenvironment caused by the formation of micelles. The CMC of the PEG_{5K}-FTS_2 micelles was determined to be 0.68 μM (Figure 3).

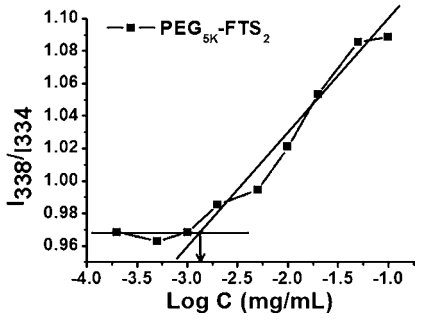

Figure 3. Plot of the ratio of I_{338}/I_{334} from fluorescence spectra as a function of logarithm concentration of PEG_{5K}-FTS_2 micelles. Pyrene was used as molecular probe ([Pyrene] = 6.0×10^{-7} M).

Table 1 shows the sizes of PTX-loaded micelles at different carrier/drug molar ratios. All of them had small size of around 20 nm. With increases in the input molar ratio of PEG_{5K}-FTS_2/PTX, the sizes of the PTX-loaded micelles were closer to that of drug-free micelles. The drug loading efficiency of PEG_{5K}-FTS_2 micelles was over 90% at various carrier/drug ratios examined (Table 1).

***In Vitro* Drug Release Study.** The profile of PTX release was examined by a dialysis method and compared to that of Taxol. For the initial 8 h, about 41.2% of PTX was released from the Taxol formulation while only 16.7% of PTX was released from the PTX-loaded PEG_{5K}-FTS_2 micelles (Figure 4). PTX release from PEG_{5K}-FTS_2 micelle formulation was significantly slower compared to Taxol formulation during the entire experimental period. The $T_{1/2}$ of PTX release is 95.4 h for PEG_{5K}-FTS_2 formulation, which is significantly longer than that for Taxol formulation (17.6 h).

Hemolytic Effect of PEG_{5K}-FTS_2 Micelles. Detrimental interaction of micelles with blood constituents such as RBCs must be avoided when these micelles are injected into the blood circulation as a carrier for drug delivery.[31] Figure 5 shows the hemolytic activities of drug free PEG_{5K}-FTS_2 micelles and polyethylenimine (PEI), a cationic polymer known to have significant hemolytic effect.[31] PEI induced hemolysis in a dose-dependent manner. In contrast, free PEG_{5K}-FTS_2 micelles did not show any detectable hemolytic activities at the same experimental concentrations, suggesting the safe profile of PEG_{5K}-FTS_2 micelles.

Western Immunoblotting. We incubated HCT-116 or 4T1.2 cells with fixed concentrations of FTS, PEG_{5K}-FTS_2(L), and PEG_{5K}-FTS_2(S) for 48 h, respectively, and the protein expression levels of Ras in the cells were examined by Western immunoblotting with pan anti-Ras Ab. As shown in Figure 6, FTS treatment caused a reduction in the total amount of cellular Ras in both cell lines. These results are consistent with the known action of FTS as a Ras inhibitor. PEG_{5K}-FTS_2(L) was comparable to free FTS in reducing the protein levels of Ras in the treated cells. In contrast, PEG_{5K}-FTS_2(S) showed minimal effect at the same FTS concentration.

***In Vitro* Cytotoxicity.** Several cancer cell lines were included in the cytotoxicity studies including murine breast cancer cells 4T1.2, human colon carcinoma cell line HCT-116, and two human prostate cancer cell lines PC-3 and DU145. Figure 7A shows the cytotoxicity of two PTX-free micelles, PEG_{5K}-FTS_2(L) and PEG_{5K}-FTS_2(S), in comparison with free FTS in 4T1.2 tumor cells. Free FTS inhibited the tumor cell growth in a concentration-dependent manner. Conjugation of FTS to PEG via a labile ester linkage resulted in only a slight decrease in antitumor activity. In contrast, a similar conjugate with a stable amide linkage [PEG_{5K}-FTS_2(S)] was significantly less active compared to both free FTS and PEG_{5K}-FTS_2 (L). A similar result was obtained in human colon cancer cells, HCT-116 (Figure 7B).

Figure 8A shows the cytotoxicity of free PTX (in DMSO) and PTX formulated in PEG_{5K}-FTS_2(L) or PEG_{5K}-FTS_2(S) micelles in 4T1.2 tumor cells. Free PTX inhibited the tumor cell growth in a concentration dependent manner. Delivery of PTX via PEG_{5K}-FTS_2(L) micelles led to a significant increase in the cytotoxicity. Interestingly, PTX formulated in PEG_{5K}-FTS_2(S) was less active than free PTX. Similar results were obtained in other tumor cell lines including DU145 (Figure 8B), PC-3 (Figure 8C), and HCT-116 (Figure 8D).

***In Vivo* Therapeutic Study.** The *in vivo* therapeutic activity of PTX formulated in PEG_{5K}-FTS_2 micelles was investigated in a syngeneic murine breast cancer model (4T1.2). As shown in Figure 9A, free PEG_{5K}-FTS_2 micelles alone showed no effects in inhibiting the tumor growth at the concentration used. The other groups treated with different PTX formulations showed varied levels of antitumor effects and they were ranked as PTX/PEG_{5K}-FTS_2(L) > PTX/PEG_{5K}-FTS_2(S) > Taxol at the same

dx.doi.org/10.1021/bc300608h | *Bioconjugate Chem.* 2013, 24, 464−472

Table 1. Physicochemical Characterization of Free Drug and PTX-Loaded PEG_{5k}-FTS_2 Micelles

micelle	molar ratio	conc. of PTX[a] (mg/mL)	size[b] (nm)	PDI[c]	DLE[d] (%)	DLC[e] (%)
PEG_{5K}-FTS_2	-	-	17.61 ± 0.9	0.201	-	-
PEG_{5K}-FTS_2:PTX	3.75:1	1	24.93 ± 1.2	0.354	90.6	3.73
PEG_{5K}-FTS_2:PTX	5:1	1	25.63 ± 3.4	0.234	97.6	2.82
PEG_{5K}-FTS_2:PTX	7.5:1	1	22.27 ± 0.6	0.268	98.0	1.90
PEG_{5K}-FTS_2:PTX	10:1	1	20.17 ± 0.2	0.189	96.2	1.43

[a]PTX concentration in micelle was kept at 1 mg/mL. Blank micelle concentration was 20 mg/mL. Values reported are the mean ± SD for triplicate samples. [b]Measured by dynamic light scattering particle sizer. [c]PDI = polydispersity index. [d]DLE = drug loading efficiency. [e]DLC = drug loading capacity.

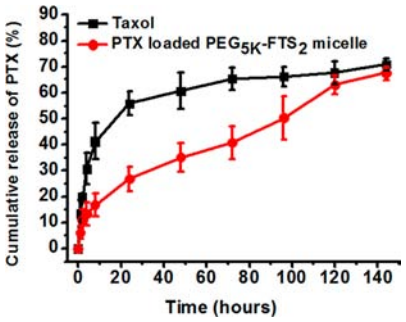

Figure 4. Cumulative PTX release profile from Taxol and PEG_{5K}-FTS_2 micelles.

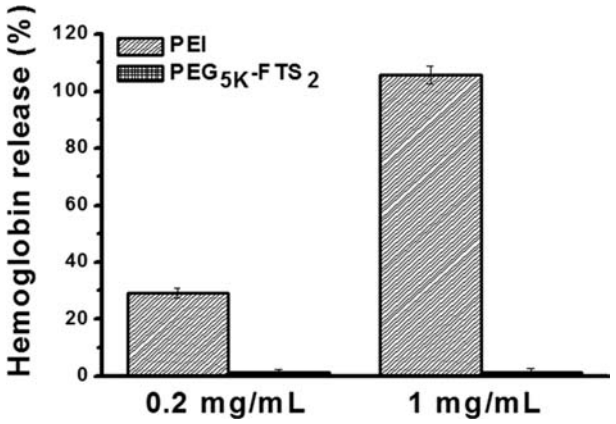

Figure 5. *In vitro* hemolysis assay of empty PEG_{5K}-FTS_2 micelles compared with PEI at two different concentrations (0.2 and 1 mg/mL). Values are reported as the mean ± SD for triplicate samples.

dose of 10 mg PTX/kg. By day 13, the relative tumor volume (RTV) was 15.1 for Taxol, while the RTVs for PTX/PEG_{5K}-FTS_2(S) and PTX/PEG_{5K}-FTS_2(L) were 13.3 and 9.6, respectively. Increasing the PTX dosage to 20 mg/kg in PTX-loaded PEG_{5K}-FTS_2(L) formulation resulted in a further improvement in antitumor activity with a RTV of 5.2. No significant changes in body weight were noticed in all treatment groups compared to PBS control group (Figure 9B).

DISCUSSION

In this study, we developed a micellar system that is based on PEG-derivatized FTS. FTS is an antagonist of Ras and is currently being evaluated as a new therapy for the treatment of various types of cancers that are associated with Ras mutations and elevated levels of Ras activity. A major feature with FTS is its excellent safety profile compared to other chemotherapeutic agents.[21,32,33] This will render PEG-FTS micelles a safe delivery system for *in vivo* delivery of various types of anticancer agents including FTS itself.

One major advantage of PEG-FTS micellar system is its very small size (~20 nm). It is generally regarded that particles in the size of 100−200 nm can be passively targeted to tumors via the leaky tumor vasculature.[34−36] However, recent studies have shown that the size of the particles needs to be below 50−60 nm for them to effectively reach the poorly vascularized tumors.[30,37] The small size of PEG-FTS micelles will allow effective passive targeting to various types of cancers including those with poorly developed tumor vasculature.

In vitro release study showed significantly slower release kinetics for PTX formulated in PEG_{5K}-FTS_2 micelles compared to Taxol formulation (Figure 4). This might be due to a more effective drug/carrier interaction for PTX/PEG_{5K}-FTS_2 mixed micelles. FTS has a benzene ring and an acyl chain. In addition to hydrophobic interaction with PTX, the $\pi-\pi$ stacking and the hydrogen bonding also contribute to the overall carrier/PTX interaction. The close proximity of two FTS molecules in PEG_{5K}-FTS_2 conjugate shall enhance the interaction of the carrier with PTX. Indeed, a PEG-FTS conjugate of 1:1 molar ratio was much less active than PEG_{5K}-FTS_2 in forming stable mixed micelles with PTX (data not shown). More studies are

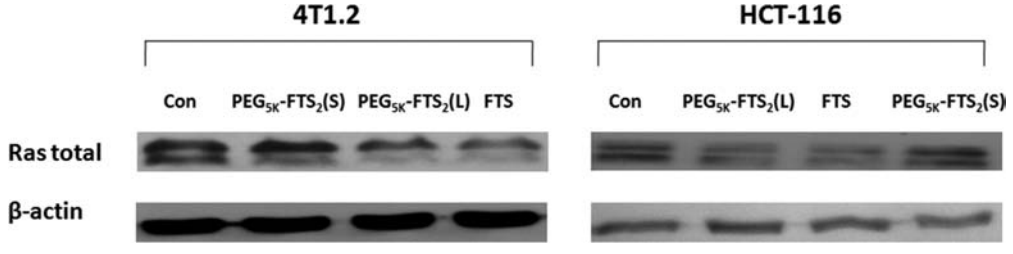

Figure 6. Effect of FTS, PEG_{5K}-FTS_2(L), andPEG_{5K}-FTS_2(S) on total Ras expression by Western blot analysis. Cells grown in medium containing 5% FBS were treated with 0.1% DMSO (control), PEG_{5K}-FTS_2(L), PEG_{5K}-FTS_2(S), and free FTS (at a FTS concentration of 10 μM), respectively, for 48 h. Total cell lysate was subjected to Western blot analysis. Anti-Ras antibody was used to determine the total Ras levels in the cells.

dx.doi.org/10.1021/bc300608h | *Bioconjugate Chem.* 2013, 24, 464−472

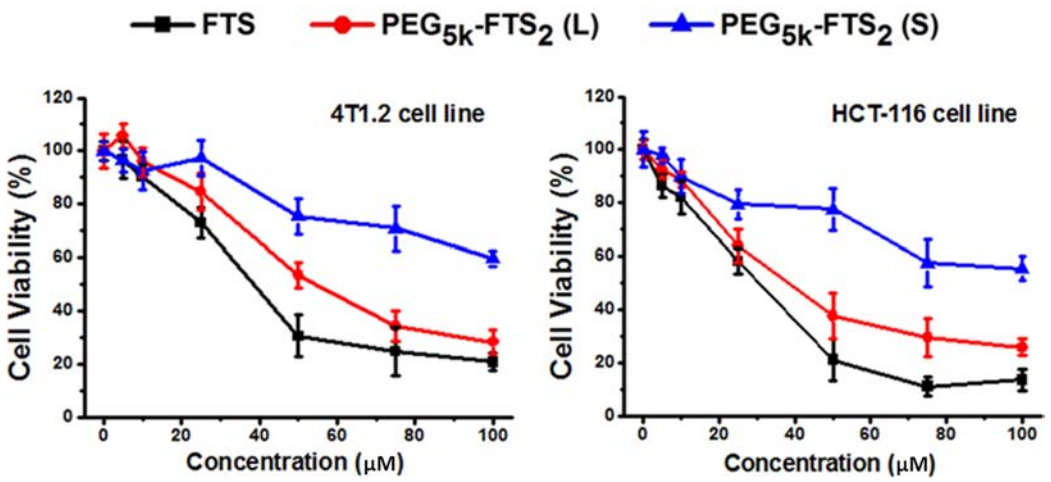

Figure 7. Cytotoxicity of free FTS, PEG_{5K}-FTS_2(L), and PEG_{5K}-FTS_2(S) in 4T1.2 mouse breast cancer cell line (A) and HCT-116 human colon carcinoma cell line (B).

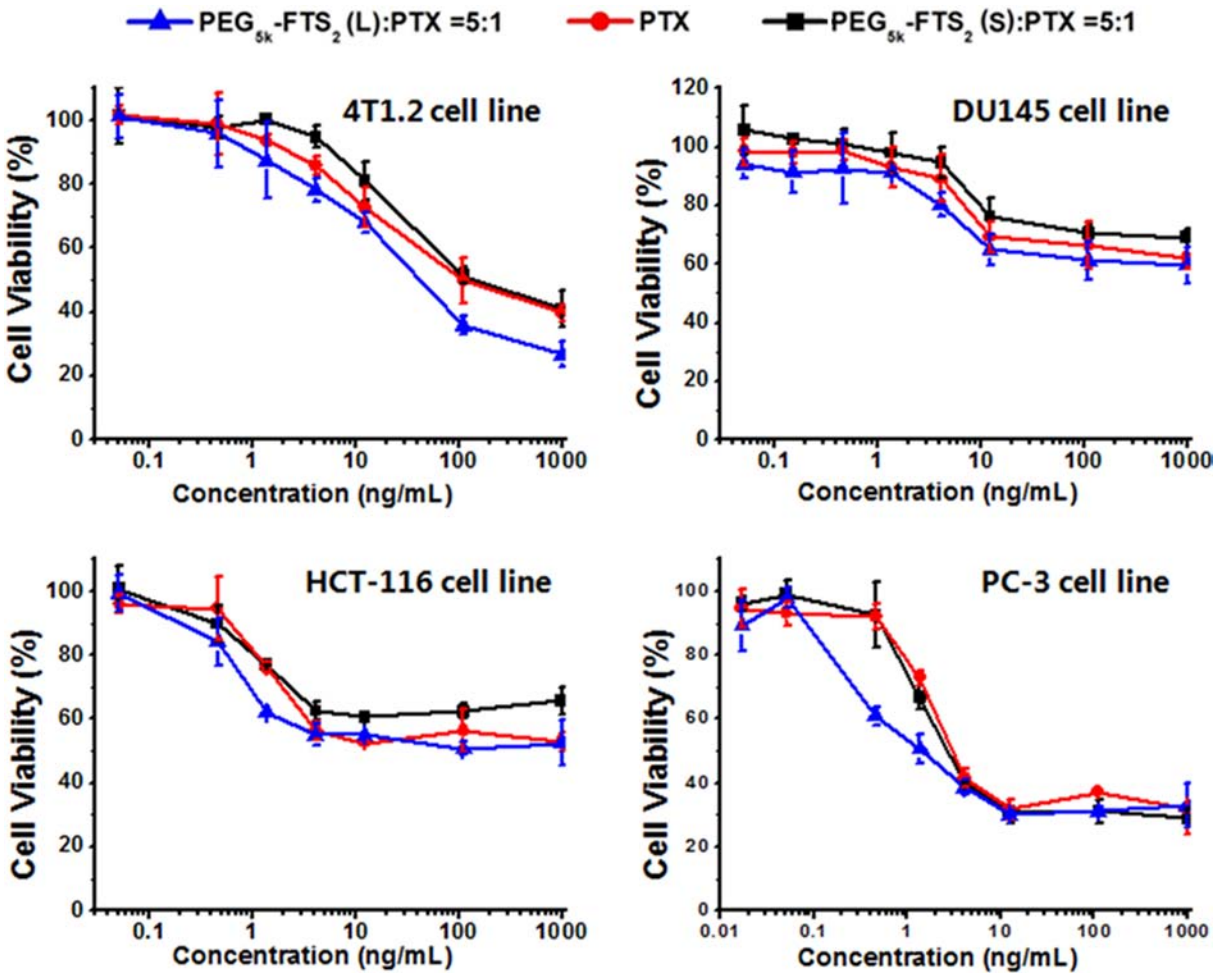

Figure 8. Cytotoxicity of free PTX, PTX/PEG_{5K}-FTS_2(L), and PTX/PEG_{5K}-FTS_2(S) against a mouse breast cancer cell line 4T1.2 (A), two androgen-independent human prostate cancer cell lines DU145 (B) and PC-3 (D), and a human colon carcinoma cell line HCT-116 (C). Cells were treated for 72 h and cytotoxicity was determined by MTT assay. Values are reported as the means ± SD for triplicate samples.

needed to better define the mechanism of drug/carrier interactions for PTX/PEG_{5K}-FTS_2 mixed micelles.

PEG_{5K}-FTS_2(L) alone was much more active than PEG_{5K}-FTS_2(S) in antitumor activity in both 4T1.2 and HCT-116 cell lines (Figure 7). It is unlikely that this is attributed to differences in the surface activity of the two conjugates, as both showed minimal hemolytic activity at the concentrations that were much higher than those used in the cytotoxicity study. It is likely that FTS is much more readily released from PEG_{5K}-FTS_2(L) by esterases following intracellular delivery. The

dx.doi.org/10.1021/bc300608h | *Bioconjugate Chem.* 2013, 24, 464−472

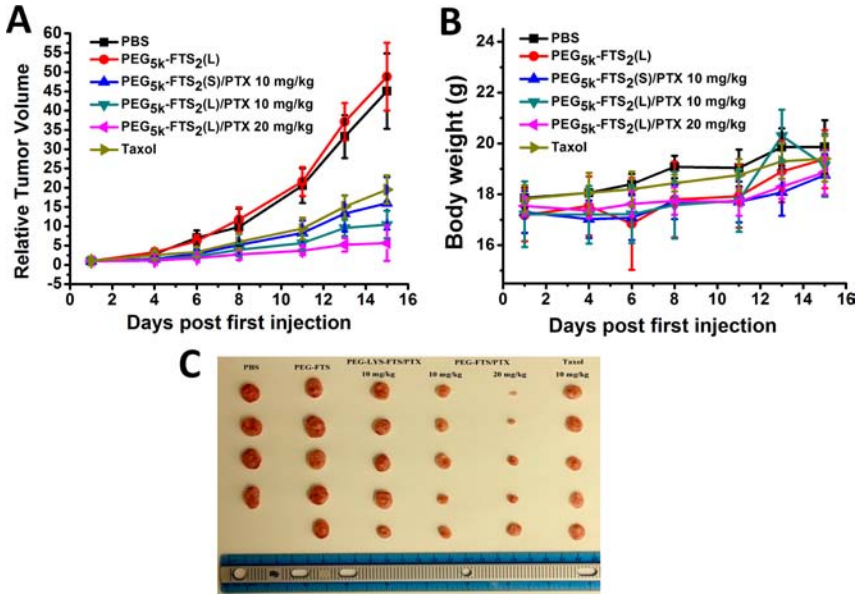

Figure 9. Enhanced antitumor activity of PTX formulated in PEG_{5K}-FTS_2(L) and PEG_{5K}-FTS(S) micelles. BABL/c mice were inoculated s.c. with 4T1.2 cells (1×10^5 cells/mouse). Five days later, mice received various treatments twice a week and tumor growth was monitored and plotted as relative tumor volume (mm^3). (A) Changes of relative tumor volume. (B) Body weight after administration. (C) The mice were sacrificed and tumors were excised from 4T1.2-bearing mice in each group. $P < 0.001$ (PTX/PEG_{5K}-FTS_2 (L) vs Taxol). $N = 5$.

cytotoxicity data agree with Western blotting in which PEG_{5K}-FTS_2(L) was more active than PEG_{5K}-FTS_2(S) in reducing the protein expression levels of Ras in treated tumor cells (Figure 6).

In addition to more potent antitumor activity by itself, PEG_{5K}-FTS_2(L) was also more active than PEG_{5K}-FTS_2(S) in mediating PTX cytotoxicity to tumor cells (Figure 8). At the concentrations used for PTX delivery, both PEG_{5K}-FTS_2(L) and PEG_{5K}-FTS_2(S) were not active in killing tumor cells by themselves. This is consistent with published works[19,38−40] and our own data (Figure 7) that FTS works at high μM concentrations. It remains to be determined if, at suboptimal concentrations as those in cells treated with PEG_{5K}-FTS_2(L), the released FTS could synergize with PTX in the overall antitumor activity. It is also possible that PTX is more readily released from PEG_{5K}-FTS_2(L) micelles due to the disintegration of the micellar system following the cleavage and release of FTS from PEG_{5K}-FTS_2(L) conjugate. More studies are needed to better understand the mechanism by which PTX/PEG_{5K}-FTS_2(L) mediated the cytotoxicity to tumor cells *in vitro*.

In vivo, PTX formulated in both PEG_{5K}-FTS_2(L) and PEG_{5K}-FTS_2(S) micelles showed better antitumor activity than Taxol formulation, although it is not statistically significant between Taxol and PTX/PEG_{5K}-FTS_2(S). This is likely due to a better stability of PEG_{5K}-FTS_2 micellar formulation as demonstrated in release study (Figure 4). Again, PTX/PEG_{5K}-FTS_2(L) was more effective than PTX/PEG_{5K}-FTS_2(S) in antitumor activity *in vivo*. It remains to be determined if similar mechanisms are involved in the improved antitumor activity for PTX/PEG_{5K}-FTS_2(L) both *in vitro* and *in vivo*.

In summary, a conjugate of PEG with two molecules of FTS forms small-sized micelles that effectively solubilize PTX. PTX formulated in this micellar system shows a PTX release kinetics that is significantly slower than that of Taxol. PEG_{5K}-FTS_2(L) conjugate retains the biological activity of FTS well, and PTX formulated in PEG_{5K}-FTS_2(L) micelles is more active in cytotoxicity than free PTX *in vitro*. *In vivo*, PTX/PEG_{5K}-FTS_2(L) shows antitumor activity that is more potent than that of Taxol or PTX/PEG_{5K}-FTS_2(S). PEG_{5K}-FTS_2(L) may represent a promising micellar system that could effectively deliver anticancer agents to tumors. Furthermore, it may potentially synergize with codelivered drugs in the overall antitumor activity.

■ ASSOCIATED CONTENT

Supporting Information

Synthesis scheme of PEG_{5K}-FTS_2(S) conjugate, ^1H NMR spectra (400 MHz) of PEG_{5K}-FTS_2(L) and PEG_{5K}-FTS_2(S) conjugates in $CDCl_3$, MALDI-TOF of PEG_{5K}-FTS_2(L) and PEG_{5K}-FTS_2(S) conjugates, and HPLC trace of PEG_{5K}-FTS_2(L) (A) and PEG_{5K}-FTS_2(S) (B) conjugates.This material is available free of charge via the Internet at http://pubs.acs.org.

■ AUTHOR INFORMATION

Corresponding Author

*Tel: 412-383-7976. Fax: 412-648-1664. E-mail: sol4@pitt.edu.

Notes

The authors declare no competing financial interest.

■ ACKNOWLEDGMENTS

This work was supported in part by NIH grants (R21CA128415 and R21CA155983) and a DOD grant (BC09603).

■ REFERENCES

(1) Goldspiel, B. R. (1997) Clinical overview of the taxanes. *Pharmacotherapy 17*, 110−125.

(2) Xie, Z., Guan, H. L., Chen, X., Lu, C., Chen, L., Hu, X., Shi, Q., and Jing, X. (2007) A novel polymer-paclitaxel conjugate based on amphiphilic triblock copolymer. *J. Controlled Release 117*, 210−216.

(3) Haag, R., and Kratz, F. (2006) Polymer therapeutics: concepts and applications. *Angew. Chem., Int. Ed. 45*, 1198−1215.

(4) Torchilin, V. P. (2007) Micellar nanocarriers: pharmaceutical perspectives. *Pharm. Res. 24*, 1−16.

(5) Tong, R., and Cheng, J. (2007) Anticancer polymeric nanomedicines. *Polym. Rev. 47*, 345−381.
(6) Maeda, H., Wu, J., Sawa, T., Matsumura, Y., and Hori, K. (2000) Tumor vascular permeability and the EPR effect in macromolecular therapeutics: a review. *J. Controlled Release 65*, 271−284.
(7) Trubetskoy, V. S. (1999) Polymeric micelles as carriers of diagnostic agents. *Adv. Drug Delivery Rev. 37*, 81−88.
(8) Riley, T., Stolnik, S., Heald, C. R., Xiong, C. D., Garnett, M. C., Illum, L., Davis, S. S., Purkiss, S. C., Barlow, R. J., and Gellert, P. R. (2001) Physicochemical evaluation of nanoparticles assembled from poly(lactic acid)-poly(ethylene glycol) (PLA-PEG) block copolymers as drug delivery vehicles. *Langmuir 17*, 3168−3174.
(9) Prencipe, G., Tabakman, S. M., Welsher, K., Liu, Z., Goodwin, A. P., Zhang, L., Henry, J., and Dai, H. J. (2009) PEG branched polymer for functionalization of nanomaterials with ultralong blood circulation. *J. Am. Chem. Soc. 131*, 4783−4787.
(10) Gref, R., Minamitake, Y., Peracchia, M. T., Trubetskoy, V., Torchilin, V., and Langer, R. (1994) Biodegradable long-circulating polymeric nanospheres. *Science 263*, 1600−1603.
(11) Croy, S. R., and Kwon, G. S. (2006) Polymeric micelles for drug delivery. *Curr. Pharm. Des. 12*, 4669−4684.
(12) Zhang, Z., and Feng, S. S. (2006) Nanoparticles of poly(lactide)/vitamin E TPGS copolymer for cancer chemotherapy: synthesis, formulation, characterization and in vitro drug release. *Biomaterials 27*, 262−270.
(13) Zhang, Z., Lee, S. H., Gan, C. W., and Feng, S. S. (2008) In vitro and in vivo investigation on PLA-TPGS nanoparticles for controlled and sustained small molecule chemotherapy. *Pharm. Res. 8*, 1925−1935.
(14) Prashant, C., Dipak, M., Yang, C. T., Chuang, K. H., Jun, D., and Feng, S. S. (2010) Superparamagnetic iron oxide–loaded poly(lactic acid)-D-alpha-tocopherol polyethylene glycol 1000 succinate copolymer nanoparticles as MRI contrast agent. *Biomaterials 21*, 5588−5597.
(15) Mi, Y., Liu, Y., and Feng, S. S. (2011) Formulation of docetaxel by folic acid-conjugated D-a-tocopheryl polyethylene glycol succinate 2000 (Vitamin E TPGS2k) micelles for targeted and synergistic chemotherapy. *Biomaterials 32*, 4058−4066.
(16) Huang, Y. H., Lu, J. Q., Gao, X., Li, J., Zhao, W. C., Sun, M., Stolz, D. B., Venkataramanan, R., Rohan, L. C., and Li, S. (2012) PEG-derivatized embelin as a dual functional carrier for the delivery of paclitaxel. *Bioconjugate Chem. 23*, 1443−1451.
(17) Lu, J. Q., Huang, Y. H., Zhao, W. C., Marquez, R. T., Meng, X. J., Li, J., Gao, X., Wang, Z., Venkataramanan, R., and Li, S. (2012) PEG-derivatized embelin as a nanomicellar carrier for delivery of paclitaxel to breast and prostate cancers. *Biomaterials,*.
(18) Nikolovska-Coleska, Z., Xu, L., Hu, Z., Tomita, Y., Li, P., Roller, P. P., Wang, R., Fang, X., Guo, R., Zhang, M., Lippman, M. E., Yang, D., and Wang, S. (2004) Discovery of embelin as a cell-permeable, small-molecular weight inhibitor of XIAP through structure-based computational screening of a traditional herbal medicine three dimensional structure database. *J. Med. Chem. 47*, 2430−2440.
(19) Haklai, R., Weisz, M. G., Elad, G., Paz, A., Marciano, D., Egozi, Y., Ben-Baruch, G., and Kloog, Y. (1998) Dislodgment and accelerated degradation of Ras. *Biochemistry 37*, 1306−1314.
(20) Marciano, D., Ben-Baruch, G., Marom, M., Egozi, Y., Haklai, R., and Kloog, Y. (1995) Selective inhibition of ras-dependent cell growth by farnesylthiosalicylic acid. *J. Med. Chem. 38*, 1267−1272.
(21) Blum, R., and Kloog, Y. (2005) Tailoring Ras-pathway—Inhibitor combinations for cancer therapy. *Drug Resistance Updates 8*, 369−380.
(22) Kloog, Y., and Cox, A. D. (2000) RAS inhibitors: potential for cancer therapeutics. *Mol. Med. Today 6*, 398−402.
(23) Gana-Weisz, M., Halaschek-Wiener, J., Jansen, B., Elad, G., Haklai, R., and Kloog, Y. (2002) The Ras inhibitor S-trans, trans-farnesylthiosalicylic acid chemosensitizes human tumor cells without causing resistance. *Clin. Cancer Res. 8*, 555−565.
(24) Rotblat, B., Ehrlich, M., Haklai, R., and Kloog, Y. (2008) The Ras inhibitor farnesylthiosalicylic acid (Salirasib) disrupts the spatiotemporal localization of active Ras: A potential treatment for cancer. *Methods Enzymol. 439*, 467−489.
(25) Paz, A., Haklai, R., Elad-Sfadia, G., Ballan, E., and Kloog, Y. (2001) Galectin-1 binds oncogenic H-Ras to mediate Ras membrane anchorage and cell transformation. *Oncogene 51*, 7486−7493.
(26) Kraitzer, A., Kloog, Y., Haklai, R., and Zilberman, M. (2011) Composite fiber structures with antiproliferative agents exhibit advantageous drug delivery and cell growth inhibition in vitro. *J. Pharm. Sci. 100*, 133−149.
(27) Zhang, P., Ye, H., Min, T., and Zhang, C. (2008) Water soluble polyethylene glycol prodrug of silybin: Design synthesis and characterization. *J. Appl. Polym. Sci. 107*, 3230−3235.
(28) Duan, K., Zhang, X. L., Tang, X. X., Yu, J. H., Liu, S. Y., Wang, D. X., Li, Y. L., and Huang, J. (2010) Fabrication of cationic nanomicelle from chitosan-graft-polycaprolactone as the carrier of 7-ethyl-10-hydroxy-camptothecin. *Colloids Surf., B: Biointerfaces 76*, 475−482.
(29) Li, Y., Xiao, K., Luo, J., Xiao, W., Lee, J. S., Gonik, A. M, Kato, J., Dong, T. A., and Lam, K. S. (2011) Well-defined, reversible disulfide cross-linked micelles for on-demand paclitaxel delivery. *Biomaterials 32*, 6633−6645.
(30) Luo, J. T., Xiao, K., Li, Y. P., Lee, J. S., Shi, L. F., Tan, Y. H., Xing, L., Cheng, R. H., Liu, G. Y., and Lam, K. S. (2010) Well-defined, size-tunable, multi-functional micelles for efficient paclitaxel delivery for cancer treatment. *Bioconjugate Chem. 21*, 1216−1224.
(31) Reul, R., Nguyen, J., and Kissel, T. (2009) Amine-modified hyperbranched polyesters as non-toxic, biodegradable gene delivery systems. *Biomaterials 30*, 5815−5824.
(32) Kloog, Y., Cox, A. D., and Sinensky, M. (1998) Concepts in Ras-directed therapy. *Expert Opin. Invest. Drugs 8*, 2121−2140.
(33) Haklai, R., Elad-Sfadia, G., Egozi, Y., and Kloog, Y. (2008) Orally administered FTS (salirasib) inhibits human pancreatic tumor growth in nude mice. *Cancer Chemother. Pharmacol. 61*, 89−96.
(34) Matsumura, Y., and Maeda, H. (1986) A new concept for macromolecular therapeutics in cancer chemotherapy: mechanism of tumouritropic accumulation of proteins and the antitumour agent smancs. *Cancer Res. 46*, 6387−6392.
(35) Maeda, H. (2001) The enhanced permeability and retention (EPR) effect in tumor vasculature: the key role of tumor-selective macromolecular drug targeting. *Adv. Enzyme Regul. 41*, 189−207.
(36) Jain, R. K. (1990) Vascular and interstitial barriers to delivery of therapeutic agents in tumors. *Cancer Metastasis Rev. 9*, 253−266.
(37) Cabral, H., Matsumoto, Y., Mizuno, K., Chen, Q., Murakami, M., Kimura, M., Terada, Y., Kano, M. R., Miyazono, K., Uesaka, M., Nishiyama, N., and Kataoka, K. (2011) Accumulation of sub-100 nm polymeric micelles in poorly permeable tumours depends on size. *Nat. Nanotechnol. 6*, 815−823.
(38) Clarke, H. C., Kocher, H. M., Khwaja, A., Kloog, Y., Cook, H. T., and Hendry, B. M. (2003) Ras antagonist farnesylthiosalicylic acid (FTS) reduces glomerular cellular proliferation and macrophage number in rat thy-1 nephritis. *J. Am. Soc. Nephrol. 14*, 848−854.
(39) Weisz, B., Giehl, K., Gana-Weisz, M., Egozi, Y., Ben-Baruch, G., Marciano, D., Gierschik, P., and Kloog, Y. (1999) A new functional Ras antagonist inhibits human pancreatic tumor growth in nude mice. *Oncogene 18*, 2579−2588.
(40) Jansen, B., Schlagbauer-Wadl, H., Kahr, H., Heere-Ress, E., Mayer, B. X., Eichler, H., Pehamberger, H., Gana-Weisz, M., Ben-David, E., Kloog, Y., and Wolff, K. (1999) Novel Ras antagonist blocks human melanoma growth. *Proc. Natl. Acad. Sci. U.S.A. 96*, 14019−14024.